

The Gowdy T^3 Cosmologies revisited

S.D. Hern and J.M. Stewart

Department of Applied Mathematics & Theoretical Physics
Silver Street Cambridge CB3 9EW

18 August 1997

Abstract

We have examined and repeated earlier numerical calculations of Berger and Moncrief for the evolution of unpolarized Gowdy T^3 cosmological models. Our calculations do not always agree with theirs, and we come to the opposite conclusion: these models do not appear to develop velocity term dominated behaviour.

DAMTP R-97/41
gr-qc/9708038

1 Introduction

The Hawking-Penrose theorems [9] imply that every “physically reasonable” cosmological model possesses a singularity; however very little is known about its nature. Early studies due to Belinskii et al. [1] suggested that the behaviour of the generic singularity resembled that of the spatially homogeneous Bianchi VIII and IX cosmological models, commonly called *mixmaster dynamics*. It is generally felt however that matters are not this simple, and attention has focussed on the *asymptotically velocity term dominated behaviour* (AVTD) hypothesis, due to Eardley et al. [5]. This claims, loosely speaking, that near the singularity, spatial derivatives are small in comparison with time derivatives; locally one has a spatially homogeneous cosmology, but the parameters vary from point to point. This is the starting point for many large-scale-structure calculations in physical cosmology, see e.g., [13], but is it correct? One needs to examine the behaviour of inhomogeneous cosmological models, and the simplest examples would appear to be the Gowdy T^3 models [6]. Polarized Gowdy cosmologies exhibit AVTD behaviour [10], and so attention focusses on the less tractable unpolarized case, which appears to require numerical treatment.

Berger & Moncrief [3] and Berger [2] (who also give a much more extensive bibliography than the brief introduction above) have tackled the unpolarized case numerically. This is a decidedly non-trivial task, and so they introduced novel numerical algorithms, which led them to conclude, tentatively, that the AVTD hypothesis was confirmed. Their grounds for caution are based on the inability of their code to resolve fine scale spatial structure. As they suggest, this problem requires an algorithm with adaptive mesh refinement (AMR), defined in section 3.

We have used our AMR code to repeat the earlier calculations. The results we obtain for the same equations and initial data used by Berger are markedly different for the calculations where spatial averaging was applied to the simulation results. Further their main conclusion, that the unpolarized Gowdy T^3 cosmologies exhibit AVTD behaviour, does not appear to be consistent with our calculations.

2 The Gowdy T^3 Universe

The line element used by Berger and Moncrief [3] for the Gowdy T^3 cosmology is

$$ds^2 = e^{\lambda/2} e^{\tau/2} (-e^{-2\tau} d\tau^2 + d\theta^2) + e^{-\tau} (e^P d\sigma^2 + 2e^P Q d\sigma d\delta + (e^P Q^2 + e^{-P}) d\delta^2), \quad (2.1)$$

where λ , P and Q are functions of τ and θ only, and $-\infty < \tau < \infty$, $0 \leq \theta, \sigma, \delta \leq 2\pi$. The functions λ , P and Q are required to be periodic in θ with period 2π . The polarized mode corresponds to $Q = 0$.

The vacuum momentum constraint equation is

$$\lambda_\theta = 2(P_\tau P_\theta + e^{2P} Q_\tau Q_\theta), \quad (2.2)$$

and the Hamiltonian constraint is

$$\lambda_\tau = P_\tau^2 + e^{-2\tau} P_\theta^2 + e^{2P} (Q_\tau^2 + e^{-2\tau} Q_\theta^2), \quad (2.3)$$

while the vacuum evolution equations reduce to

$$P_{\tau\tau} = e^{-2\tau} P_{\theta\theta} + e^{2P} (Q_\tau^2 - e^{-2\tau} Q_\theta^2), \quad (2.4)$$

$$Q_{\tau\tau} = e^{-2\tau} Q_{\theta\theta} - 2(P_\tau Q_\tau - e^{-2\tau} P_\theta Q_\theta). \quad (2.5)$$

Here $f_\tau = \partial f / \partial \tau$ etc. It should be noticed that the evolution equations are unconstrained; they do not involve λ . The energy constraint (2.3) determines λ and the momentum constraint (2.2) is satisfied at all times if it is satisfied initially, provided the other equations hold. As pointed out by Berger & Moncrief [3] the evolution equations are harmonic map equations for a target space with metric

$$dS^2 = dP^2 + e^{2P} dQ^2, \quad (2.6)$$

and so study of these equations is not without interest.

The integration programmes described in the next section require a first order system of equations. We accomplish this by introducing new variables as follows

$$A = P_\tau, \quad B = Q_\tau, \quad C = P_\theta, \quad D = Q_\theta. \quad (2.7)$$

The evolution equations now take the form

$$A_\tau = e^{-2\tau} C_\theta + e^{2P} (B^2 - e^{-2\tau} D^2), \quad (2.8a)$$

$$B_\tau = e^{-2\tau} D_\theta - 2(AB - e^{-2\tau} CD), \quad (2.8b)$$

$$C_\tau = A_\theta, \quad (2.8c)$$

$$D_\tau = B_\theta, \quad (2.8d)$$

$$P_\tau = A, \quad (2.8e)$$

$$Q_\tau = B. \quad (2.8f)$$

Initial data at $\tau = 0$ is also required. Berger & Moncrief suggested that the following choice was reasonably generic

$$A = v_0 \cos \theta, \quad B = 0, \quad C = 0, \quad D = -\sin \theta, \quad P = 0, \quad Q = \cos \theta, \quad (2.9)$$

and the results reported here use $v_0 = 10$ as used in [3].

3 Numerical Procedures

As we shall see in the next section, the evolution produces structure on fine scales with steep gradients. One numerical strategy is to use a standard algorithm e.g., Lax-Wendroff, together with a very fine grid structure. This certainly works but it is not the most efficient way to proceed. Berger & Moncrief [3] used a *symplectic integrator*, described in their paper. However their calculation produced fine scale structure even at sizes comparable with the grid spacing, which they regarded as unreliable. In presenting their results spatial averaging was used to remove the finest scale structure. An alternative approach is due to van Putten [12], but he reports integration of the equations only for short times and small values of the parameter v_0 in the initial data.

Problems of this type are natural candidates for adaptive mesh refinement (AMR), which seeks to add extra grid points when they are needed and to remove them when they become unnecessary. We used an implementation of the Berger & Oliger [4] AMR algorithm which is based on that described in Hamadé & Stewart [8]. Numerous changes have been made to that code. Those relevant to this paper are:

- an arbitrary number of grids may exist at each level of refinement,
- it is now possible to switch in arbitrary integrators, giving the code “modularity”,
- cubic spline interpolation is preferred to the quadratic interpolation used earlier, thus guaranteeing continuous spatial second derivatives,
- when creating finer grids one can choose whether to use data from obsolete grids at the same level, rather than relying on interpolation from the parent grid.

For non-specialists, the third change introduces a subtle form of data smoothing, which can be (almost) eliminated by the fourth change.

It is straightforward to write a generalization of the standard Lax-Wendroff two step algorithm which is second order accurate for the system (2.8), and this proved to be the fastest choice. (If the typical spatial grid spacing is Δx , then a second order accurate method produces a local truncation error which is $O((\Delta x)^3)$. The mesh refinement is typically $\Delta x \rightarrow \Delta x/4$, and so a single stage of refinement reduces the local truncation error by nearly two orders of magnitude, as well as enhancing spatial resolution.) In addition (and as part of a long term programme) we used our interpretation of the second order accurate wave propagation routine from the CLAWPACK high resolution package of LeVeque [11]. (CLAWPACK is written in FORTRAN. The administrative part of our code is written in C++, and the numerically intensive functions are written either in C or C++. It proved easier, and more instructive, to adapt the CLAWPACK routines to this environment, rather than to interface the FORTRAN to the existing code.)

For calculations using the Berger-Oliger algorithm the initial coarse grid had a spatial separation $\Delta x = 2\pi/2000$. The finest child grid actually used had $\Delta x = 2\pi/512000$. As a check to ensure that the AMR code was not introducing spurious effects we repeated the calculations with $\Delta x = 2\pi/8000$ and no mesh refinement. The Lax-Wendroff and CLAWPACK-like codes were developed by the two different authors, continuing our policy to eliminate coding errors. We also checked our codes against the exact pseudo-unpolarized solution

$$P = \log \cosh P_0, \quad Q = \tanh P_0, \quad P_0(\tau, \theta) = Y_0(e^{-\tau}) \cos \theta, \quad (3.1)$$

(where Y_0 is a Bessel function) given by Berger & Moncrief [3]. There were only very small differences between the results from the various runs. What is reported in the next section is common to all of them.

4 Numerical Results

We are reporting on the integration of equations (2.8) with initial data (2.9), the same data as that used by Berger & Moncrief [3]. (If we decrease the parameter v_0 less spatial structure occurs, while increasing v_0 produces more structure.)

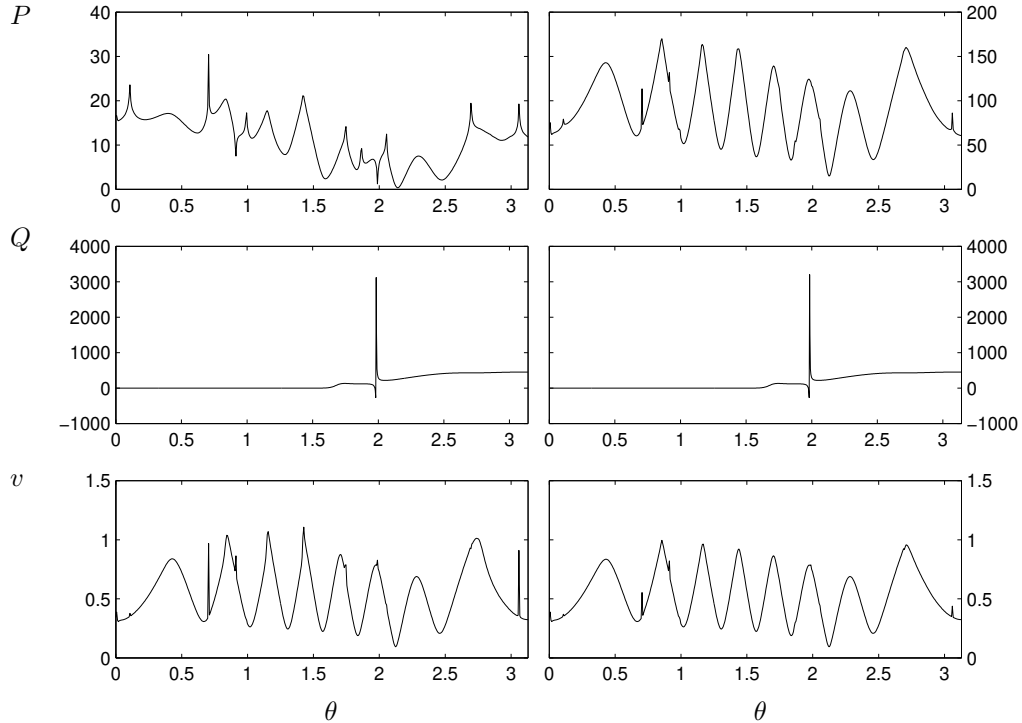


Figure 1: P , Q and v as functions of θ at two different times. The left column corresponds to $\tau = 6\pi$ and θ ranges from 0 to π . The right column corresponds to $\tau = 54\pi$. (The figures are all symmetric under $\theta \rightarrow 2\pi - \theta$, and so only one half of the θ -range is shown.)

Their main results are summarized in figures 4–6 of [3]. The left column of our figure 1 shows P , Q and $v = \sqrt{P_\tau^2 + \exp(2P)Q_\tau^2}$ as functions of θ at $\tau = 18.85$, the latest time of their figures 4–6. The behaviour of P is very different with a number of fine spikes which are not present in the earlier figures which use spatial averaging in displaying the results. Berger also displayed calculations without using spatial averaging, and obtained sharp spikes in P . This effect is discussed in [2], where it is asserted that the spikes occur at turning points of Q , i.e., where $D = Q_\theta = 0$. Our results do not wholly concur with this statement. The majority of P -spikes occur at zeros of D . However we have found spikes forming where $D \neq 0$, and zeros of D where spikes do not form.

In order to suggest reliable reasons for the observed behaviour it is necessary to understand which are the dominant terms in the governing equations. Here we adopt the definition that a term is *dominant* if its absolute value exceeds ten times the absolute value of the sum of the other terms. Figure 2 illustrates this for the wave equations (2.8a, b) for $A_\tau = P_{\tau\tau}$ and $B_\tau = Q_{\tau\tau}$. (Note that this problem is invariant under $\theta \rightarrow 2\pi - \theta$ and so only half of the θ -range is shown.) The lightly shaded regions in (τ, θ) space are where the terms $\exp(2P)B^2$ (in (2.8a)) and $-2AB$ (in (2.8b)) dominate the right hand sides. The darker shaded regions are where the terms $-\exp(2P - 2\tau)D^2$ and $2\exp(-2\tau)CD$ are the dominant ones. There are some narrow black regions where the spatial derivative terms $\exp(-2\tau)C_\theta$ and $\exp(-2\tau)D_\theta$ dominate the equations. The white regions are where there are no dominant terms. It is obvious from the figure that the evolution of A , and hence of P , is a very complicated process and so it is unlikely that spike formation has a simple

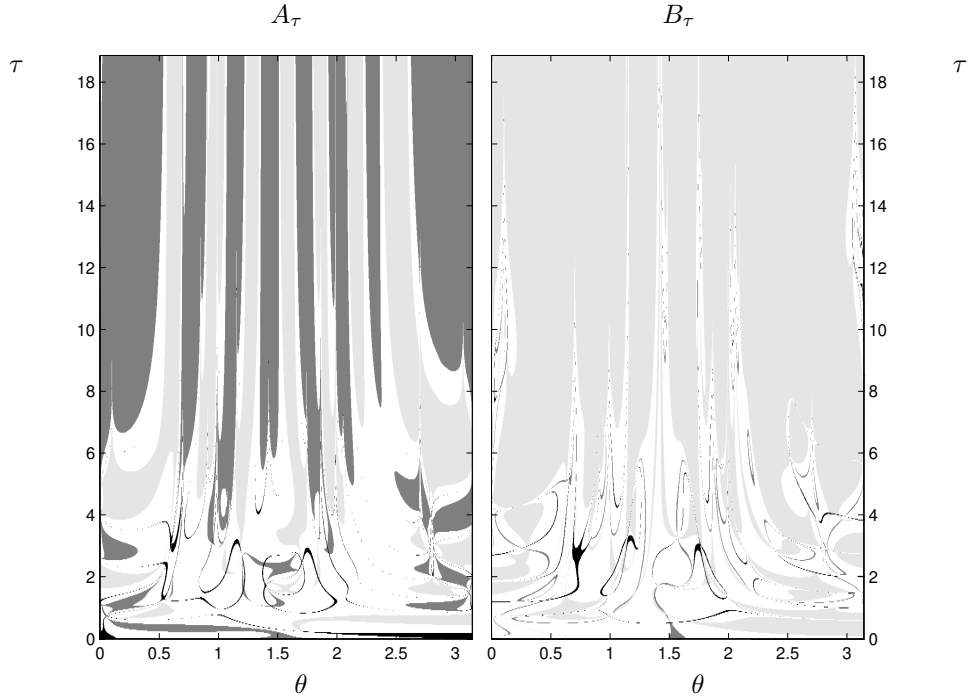


Figure 2: The dominant terms in the A_τ and B_τ equations (2.8a,b) as functions of θ and τ . The black regions are where the C_θ and D_θ terms dominate. The dark shaded regions are where terms involving C and D dominate, and the light shaded regions are where the terms involving A and B dominate. In the white regions no one term dominates.

cause.

The behaviour of Q on the left hand side of figure 1 is even more striking. Near $\theta = 2$, Q dips suddenly to a value of about -300 , before rising to 3000 and then resuming smoother behaviour. The absolute value of the gradient $|Q_\theta|$ is about 2.5×10^6 there. This effect is also reported in [2], see especially figure 2 there (but the position and scale are different, because they were calculated for $v_0 = 5$ rather than the value of 10 used in [3] and here). Further the explanation given there is not quite correct. A close examination of figure 2 reveals that the region around $\theta = 2$, $4 < \tau < 6$ is light grey for both equations. From this we may conclude that in this region the terms proportional to $\exp(-2\tau)$ are irrelevant so that we have

$$A_\tau \approx e^{2P} B^2, \quad B_\tau \approx -2AB. \quad (4.1)$$

To form the apparent discontinuity we need the conditions of a zero in B (which can be seen as a narrow white region in both halves of figure 2) with both A and P negative. Then $A_\tau > 0$ and is small, so that A and P remain negative. Because of this, on either side of the zero, B will grow exponentially, but with opposite sign, and the same obviously happens to Q . (At the zero of B , (4.1) doesn't strictly apply but it is a reasonable approximation.) Since $A_\tau > 0$ the region in which $A < 0$ narrows, steepening the slope of Q . Eventually $A > 0$, so that B decreases exponentially, and this ends spike formation.

AVTD behaviour requires that the spatial derivative terms in equations (2.4), (2.5) be negligible, or equivalently that the terms $\exp(2P)B^2$ and $-2AB$ dominate the right hand sides of equations (2.8a), (2.8b) respectively. Thus AVTD behaviour corresponds to the intersections of the lightly shaded regions in figure 2. Clearly this behaviour has not been reached at time $\tau = 6\pi = 18.85$. There is a conjecture that AVTD behaviour requires $v < 1$ for almost all θ [7]. Examination of the bottom left graph of figure 1 shows regions where $v > 1$ at this time.

We carried the integration further to $\tau = 54\pi$, by which time $v < 1$ everywhere. Plots of P , Q

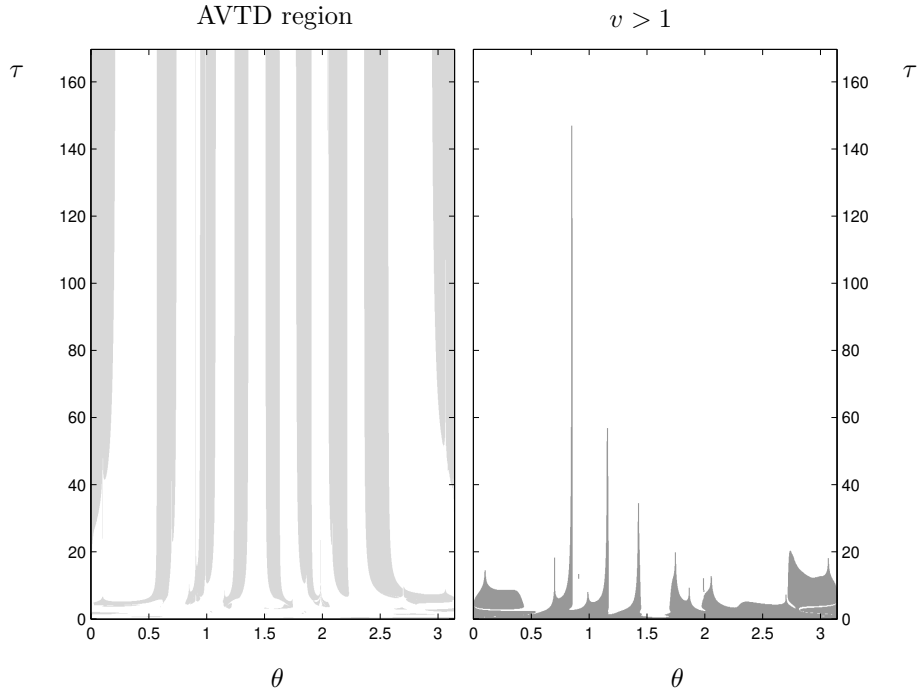


Figure 3: In the left half the grey regions show those points where the spatial derivative terms in equations (2.8) are negligible. The grey regions in the right figure are where $v > 1$.

and v as functions of θ at this time are given in the right hand column of figure 1. The spikes in P have softened slightly, which may be a numerical effect. We find that $P \approx v\tau$ and $B = Q_\tau \approx 0$ consistent with AVTD behaviour.

In the left half of figure 3, the regions where the terms $\exp(2P)B^2$ and $-2AB$ dominate equations (2.8a,b) are shaded. There are distinct ranges of θ where AVTD behaviour does not occur, and they do not appear to be shrinking as τ increases. Careful examination of the left half of figure 3 and the graph of v at $\tau = 54\pi$ in figure 1 shows that the regions of AVTD behaviour correspond precisely to the minima of v whereas regions where AVTD behaviour does not occur correspond to the maxima of v . Figure 1 also shows that at late time we appear to have $v < 1$ for all values of θ . The right half of figure 3 shows the regions in (τ, θ) space where $v > 1$, and contrasts with figure 9 of [3] where $v < 1$ everywhere is found at much earlier times.

Thus we conclude that the AVTD hypothesis is probably invalid for this model. It is certainly true that the spatial derivative terms become small, but so does $B = Q_\tau$, and for certain regions of θ the term without spatial derivatives $\exp(2P)B^2$ in equation (2.8a) fails to dominate the right hand side of that equation. It is perhaps worth noting that whatever terms dominate, the right hand sides of equations (2.8a,b) are becoming exponentially small. Thus the behaviour is very much what one would have expected of an AVTD model. Perhaps the definition needs to be reformulated.

5 Conclusions

We have been unable to confirm the main result of Berger & Moncrief [3] for a particular, but hopefully generic, choice of initial data: the unpolarized Gowdy T^3 cosmological models exhibit AVTD behaviour. This is because there are major discrepancies between their calculations and ours. The older calculations which used spatial averaging in the presentation of the results have discarded the finest scale structure of the solutions. (Some later calculations [3], [2] did not introduce averaging and obtained the spikes and steep gradients reported here. In particular we

have performed the evolution leading to figure 2 of [2] and can confirm its accuracy.)

We have looked carefully at what are the dominant terms in the equations for any given region of (τ, θ) space. Even at times as late as $\tau = 54\pi$, somewhat longer than the evolution described in [3], there are ranges of θ where the spatial derivative terms are not negligible. That is to say, the remaining “velocity terms” do not dominate the equations in the sense defined in section 4. Further this analysis has led us to disagree with or modify some of the explanations for fine scale structure given by Berger & Moncrief.

We have not investigated in detail the symplectic integrator they used, but for this problem at least it would seem to be unnecessary. As reported in section 3, one does not even need an AMR code. The problem can be handled with a simple Lax-Wendroff code with about 8000 grid points, and although this procedure is slower than our AMR code, it gives essentially the same results. However the AMR code has for this problem several distinct advantages:

- speed,
- one has no reliable prediction as to whether more fine scale spatial structure will appear, e.g., evolutions with larger values of v_0 produce more spatial structure and require much more refinement,
- at late times the spatial structure “freezes” and very little refinement is required.

We thank Neil Cornish for useful discussions. Simon Hern was supported by an EPSRC studentship.

References

- [1] V.A. Belinskii, I.M. Khalatnikov & E.M. Lifschitz, *Advances in Physics*, **19**, 525 (1970); *ibid.* **31**, 639 (1982).
- [2] B.K. Berger, in *Proceedings of the 14th International Conference on General Relativity and Gravitation*, edited by M. Francaviglia et al., World Scientific (1997).
- [3] B.K. Berger & V. Moncrief, *Phys. Rev.*, **D48**, 4676 (1993).
- [4] M.J. Berger & J. Oliger, *J. Comp. Phys.*, **53**, 484 (1984).
- [5] D. Eardley, E. Liang & R. Sachs, *J. Math. Phys.*, **13**, 99 (1972).
- [6] R.H. Gowdy, *Phys. Rev. Lett.*, **27**, 826 (1971); *ibid.* **27**, E1102 (1971); *Ann. Phys. (NY)*, **83**, 203, (1974).
- [7] B. Grubišić & V. Moncrief, *Phys. Rev.*, **D47**, 2371 (1993).
- [8] R. Hamadé & J.M. Stewart, *Classical & Quantum Gravity*, **13**, 497 (1996).
- [9] S.W. Hawking & G.F.R. Ellis, *The large scale structure of space-time*, Cambridge (1973).
- [10] J. Isenberg & V. Moncrief, *Ann. Phys. (NY)*, **199**, 84 (1990).
- [11] R.J. LeVeque, *J. Comp. Phys.*, **131**, 327 (1997).
- [12] M.H.P.M. van Putten, *Phys. Rev.*, **D55**, 4705 (1997).
- [13] D.S. Salopek & J.M. Stewart, *Phys. Rev.*, **D51**, 517 (1995).